



Nuclear Data Needs for Accelerator Driven Transmutation System

K. Tsujimoto, T. Sasa, H. Takano, T. Nakagawa

Japan Atomic Energy Research Institute, Japan

Abstract

The accelerator-driven transmutation system has been studied at the Japan Atomic Energy Research Institute. This system is a hybrid system which consists of a high intensity accelerator, a spallation target and a subcritical core region. Nuclides in high-level waste to be transmuted are minor actinides and long-lived fission products which are loaded in subcritical core and blanket in ADS, respectively. The calculations of subcriticality and burnup swing by present evaluated nuclear data were performed to investigate the effect on the performance of ADS. To compare with the integrated experimental and calculational results, analyses of actinide samples irradiated in the Dounreay Prototype Fast Reactor are presented. Recent measurements for thermal neutron capture cross section which affect transmutation efficiency are shown compared with evaluated nuclear data for some long-lives fission products.

1 Introduction

The Japanese long-term program called OMEGA has started in 1988 for research and development of new technologies for partitioning and transmutation of minor actinides and fission products. The main aims of this program are exploring the possibility to utilize high-level waste as useful resources and widening options of future waste management. Further improvements of long-term safety assurance in the waste management can be expected through establishing the partitioning and transmutation technology. Under the OMEGA Program, the Japan Atomic Energy Research Institute (JAERI) is proceeding with the research and development on proton accelerator-driven system (ADS).¹ Nuclides in high-level waste to be transmuted are minor actinides (MA) and long-lived fission products (LLFP). Transmutation of MA and LLFP was studied by using a lead-bismuth cooled ADS with 800MWth.² MA should be transmuted mainly through fission reactions because the transmutation of MA by neutron capture reactions has the possibility of increasing higher actinides, while the thermal capture is main transmutation reaction for LLFP. The mixture of the mono-nitride of plutonium and MA and inert matrix is used as the fuel for the subcritical fuel region surrounding the spallation target is driven by the spallation neutrons. It is possible to transmute LLFP in a thermalized region surrounding subcritical fuel region. The concepts for Pb-Bi cooled ADS are shown in Fig. 1.

The transmutation of MA and the burnup reactivity swing are especially important to estimate the performance of ADS. Nuclear data about MA is directly connected these characteristics. Fission and capture cross sections are dominant factor in transmutation and subcriticality of ADS. Neutron yield per fission and fission spectrum are also important in estimating of k-eff. The delayed neutron data which connects to operating and monitoring of subcritical level in ADS is one of important factor. For LLFP, accuracy of nuclear data affect transmutation efficiency because these nuclides are transmuted to stable nuclide by neutron absorption reaction.

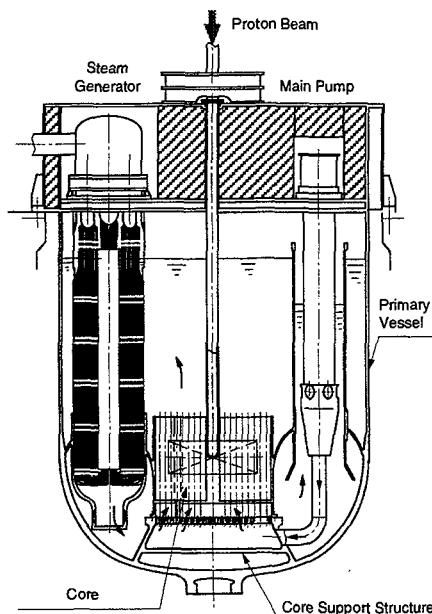


Fig. 1 Preliminary design of Pb-Bi cooled ADS plant

The effect of nuclear data for characteristics of ADS including present status of nuclear data about MA and LLFP are discussed following section.

2 Effect of Nuclear Data on Characteristics of ADS

In ADS, plutonium and MA from power reactor are used as a fuel of subcritical core. Typical plutonium and MA compositions resulting from reprocessing of UO_2 and MOX fuel from PWR are showed in Table 1.³ In all cases which are considered, seven years cooling times before reprocessing. The most different nuclide between MA from UO_2 and MOX fuel PWR is ^{237}Np . ^{237}Np is mainly produced from ^{235}U , so in MOX fuel with depleted uranium it produce less amount of ^{237}Np . These nuclides becomes initial loading fuel in ADS.

The accuracy of subcriticality and burnup swing are very important factor in ADS. The system must be subcritical in any case since ADS is driven with spallation neutron source by proton beam. The proton beam power needed to operate the ADS is connected to the multiplication factor (k -eff) of system, if the initial k -eff is 0.95, the burnup swing of 2% is corresponds to the proton beam swing of about 50%. Therefore, the minimization of the burnup swing is an important factor in operation of ADS. To investigate the effect of nuclear data on k -eff and burnup swing in ADS, burnup calculations are carried out using the ATRAS code system⁴ with the JENDL-3.2, ENDF/B-VI and JEF-2.2 libraries, respectively. The burnup characteristics were investigated for ADS loading plutonium and MA from UO_2 and MOX fuel PWR with 50 GWd/t burnup. We assumed initial Pu loading as 40% for both cores because the burnup reactivity swing is minimized in the core with the initial Pu loading of 40%. The burnup calculations were done for five burnup cycles which was constructed by the burnup of two years and the cooling of three years. In the cooling period, the fission products were removed and the fresh fuel of equal mass to the fission products was added to the burnup fuel. The additional fresh fuel contained MA only, so Pu was loaded only once at the initial loading. The burnup swings in initial two years operation are showed in Fig. 2. The results show large discrepancy of about 1% for k -eff at initial core. The burnup swings, especially for Pu and MA from MOX

Table 1 Plutonium and MA compositions resulting from reprocessing of UO₂ and MOX fuel from PWR (nuclide atom %)³

| Fuel | UO ₂ | UO ₂ | MOX | MOX |
|-------------------|-----------------|-----------------|----------|----------|
| Burnup | 33 GWd/t | 50 GWd/t | 33 GWd/t | 50 GWd/t |
| ²³⁸ Pu | 1.5 | 2.7 | 2.6 | 4.1 |
| ²³⁹ Pu | 59.3 | 55.3 | 44.5 | 41.9 |
| ²⁴⁰ Pu | 23.7 | 23.9 | 31.0 | 30.5 |
| ²⁴¹ Pu | 8.7 | 9.5 | 10.7 | 10.6 |
| ²⁴² Pu | 5.5 | 7.1 | 9.5 | 11.3 |
| ²⁴¹ Am | 1.3 | 1.5 | 1.7 | 1.7 |
| Total | 100 | 100 | 100 | 100 |
| ²³⁷ Np | 44.6 | 46.4 | 4.5 | 4.4 |
| ²⁴¹ Am | 43.6 | 37.1 | 62.5 | 58.3 |
| ²⁴³ Am | 9.7 | 12.7 | 24.3 | 26.1 |
| ²⁴⁴ Cm | 2.1 | 3.8 | 8.7 | 11.3 |
| Total | 100 | 100 | 100 | 100 |

fuel PWR, also show different trend.

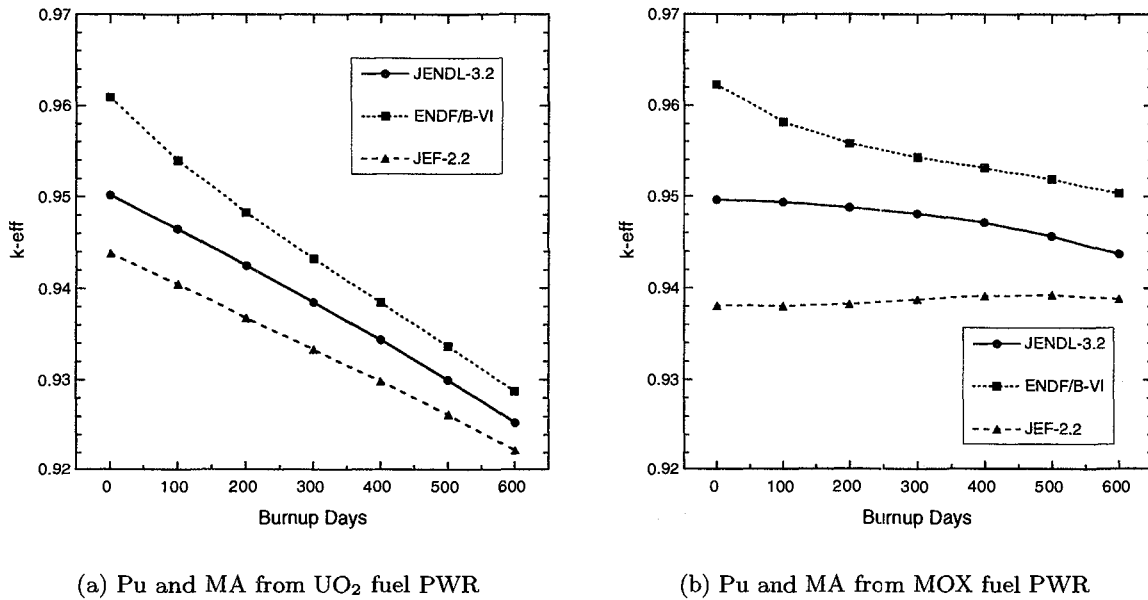


Fig. 2 Comparison of burnup swing during 600 days operation for ADS with fuel from UO₂ and MOX fuel PWR

To investigate the reason of discrepancy among results by different nuclear data, nuclides and reaction contributions for difference of k-eff at initial core were calculated by perturbation calculations. The results for MA from UO₂ fuel PWR at beginning of cycle (BOC) and end of cycle (EOC) are showed in Table 2 and Table 3, respectively. The values at BOC reflect the difference of nuclear data, but those at EOC include the difference of change in amount of each nuclides. The results show that contributions of capture reaction and neutron yield

are large while fission reaction seem to be smaller. The contributions of ^{237}Np and ^{241}Am between JENDL-3.2 and ENDF/B-VI, ^{241}Am between JENDL-3.2 and JEF-2.2 are dominant in the differences in capture reaction at BOC. For ^{237}Np , the differences in capture reaction in Table 2 indicates that evaluated value in JENDL-3.2 is different from other nuclear data. The capture cross section affect the burnup swing because capture reaction of ^{237}Np , ^{241}Am and ^{244}Cm produce ^{238}Pu , ^{242m}Am and ^{245}Cm which has relatively high fission cross section. ^{241}Am capture cross sections and energy break down of differences in capture reaction between nuclear data are showed in Fig. 3. It indicates that the energy region above 1 keV is dominant and contribution of capture reaction on k-eff is very sensitive to the difference of cross section. For neutron yield, the contributions of ^{243}Am and ^{241}Pu between JENDL-3.2 and ENDF/B-VI, ^{237}Np and ^{239}Pu are relatively large at BOC. The contribution of secondary produced MA, such as ^{238}Pu , ^{242m}Am and ^{245}Cm , become large with burnup. For the comparison between JENDL-3.2 and ENDF/B-VI, the difference in ^{242}Cm is large. This is because, in the evaluation of ENDF/B-VI, the fission cross section in the resonance region for ^{242}Cm is too small as shown in Fig. 4. This is one of the reason for difference of burnup swing. The branching ratio of $^{241}\text{Am}(n,\gamma)^{242g}\text{Am}$ and $^{241}\text{Am}(n,\gamma)^{242m}\text{Am}$ reactions is important. Its evaluated data, however, are only given in ENDF/B-VI, so a constant value of 0.8 for isomeric ratio of $^{241}\text{Am}(n,\gamma)^{242g}\text{Am}$ and total capture reaction was used for all calculations. A comparison with the evaluated and experimental data is showed in Fig. 5.^{5,6} The data in the thermal region are satisfactory, but it is necessary to investigate in the higher energy region.

Table 2 Nuclides and reaction component for difference of initial k-eff in ADS with Pu and MA from UO_2 fuel PWR (% $\Delta k/k$)

| Comparison between JENDL-3.2 and ENDF-B-VI | | | | | |
|--|--------|------------|------------|------------|---------------|
| | Total | Σ_c | Σ_f | Σ_s | $\nu\Sigma_f$ |
| ^{237}Np | 0.453 | 0.254 | 0.112 | 0.020 | 0.066 |
| ^{238}Pu | -0.041 | -0.025 | 0.005 | -0.009 | -0.011 |
| ^{239}Pu | 0.038 | 0.116 | 0.018 | 0.011 | -0.107 |
| ^{240}Pu | 0.287 | 0.135 | -0.019 | 0.051 | 0.120 |
| ^{241}Pu | -0.158 | 0.054 | 0.032 | -0.052 | -0.190 |
| ^{242}Pu | -0.001 | 0.024 | -0.001 | -0.003 | -0.021 |
| ^{241}Am | 0.225 | 0.332 | 0.002 | -0.077 | -0.032 |
| ^{243}Am | 0.347 | 0.187 | -0.056 | -0.089 | 0.304 |
| ^{244}Cm | 0.019 | -0.070 | -0.005 | -0.019 | 0.113 |
| Total | 1.170 | 1.008 | 0.087 | -0.167 | 0.241 |

| Comparison between JENDL-3.2 and JEF-2.2 | | | | | |
|--|--------|------------|------------|------------|---------------|
| | Total | Σ_c | Σ_f | Σ_s | $\nu\Sigma_f$ |
| ^{237}Np | 0.104 | 0.257 | 0.136 | 0.157 | -0.445 |
| ^{238}Pu | 0.005 | 0.023 | 0.003 | -0.009 | -0.013 |
| ^{239}Pu | 0.364 | -0.038 | -0.129 | -0.007 | 0.537 |
| ^{240}Pu | 0.109 | 0.037 | -0.030 | -0.007 | 0.107 |
| ^{241}Pu | -0.158 | -0.122 | 0.006 | -0.011 | -0.034 |
| ^{242}Pu | -0.008 | 0.003 | -0.004 | 0.015 | -0.021 |
| ^{241}Am | -0.989 | -1.441 | 0.079 | 0.278 | 0.095 |
| ^{243}Am | -0.106 | -0.247 | -0.036 | 0.144 | 0.033 |
| ^{244}Cm | 0.060 | 0.060 | -0.010 | -0.012 | 0.021 |
| Total | -0.619 | -1.466 | 0.016 | 0.550 | 0.281 |

Table 3 Nuclides and reaction component for difference of k-eff at end of cycle in ADS with Pu and MA from UO₂ fuel PWR (%Δk/k)

| Comparison between JENDL-3.2 and ENDF-B/VI | | | | | |
|--|--------|------------|------------|------------|---------------|
| | Total | Σ_c | Σ_f | Σ_s | $\nu\Sigma_f$ |
| ²³⁷ Np | 0.391 | 0.222 | 0.071 | 0.013 | 0.086 |
| ²³⁸ Pu | -0.333 | -0.173 | 0.053 | -0.059 | -0.154 |
| ²³⁹ Pu | 0.039 | 0.087 | -0.007 | 0.008 | -0.063 |
| ²⁴⁰ Pu | 0.337 | 0.157 | -0.031 | 0.049 | 0.162 |
| ²⁴¹ Pu | -0.274 | 0.047 | 0.065 | -0.037 | -0.350 |
| ²⁴² Pu | 0.003 | 0.036 | -0.001 | -0.006 | -0.046 |
| ²⁴¹ Am | 0.198 | 0.278 | 0.001 | -0.057 | -0.023 |
| ^{242m} Am | 0.658 | 0.045 | -0.116 | 0.021 | 0.708 |
| ²⁴³ Am | 0.298 | 0.157 | -0.048 | -0.071 | 0.259 |
| ²⁴² Cm | -0.880 | 0.052 | 0.252 | -0.043 | -1.141 |
| ²⁴³ Cm | -0.089 | 0.003 | 0.018 | -0.002 | -0.108 |
| ²⁴⁴ Cm | -0.036 | -0.088 | 0.018 | -0.023 | 0.057 |
| ²⁴⁵ Cm | 0.134 | -0.002 | -0.023 | -0.014 | 0.173 |
| Total | 0.445 | 0.819 | 0.266 | -0.219 | 0.421 |

| Comparison between JENDL-3.2 and JEF-2.2 | | | | | |
|--|--------|------------|------------|------------|---------------|
| | Total | Σ_c | Σ_f | Σ_s | $\nu\Sigma_f$ |
| ²³⁷ Np | 0.106 | 0.152 | 0.057 | 0.106 | -0.209 |
| ²³⁸ Pu | 0.150 | 0.191 | -0.006 | -0.060 | 0.025 |
| ²³⁹ Pu | 0.082 | -0.010 | -0.041 | -0.000 | 0.133 |
| ²⁴⁰ Pu | 0.128 | 0.041 | -0.035 | -0.010 | 0.132 |
| ²⁴¹ Pu | -0.261 | -0.081 | 0.042 | -0.006 | -0.216 |
| ²⁴² Pu | 0.008 | -0.010 | -0.021 | 0.028 | 0.022 |
| ²⁴¹ Am | -0.678 | -0.827 | 0.130 | 0.219 | -0.200 |
| ^{242m} Am | 0.279 | -0.001 | -0.080 | -0.019 | 0.379 |
| ²⁴³ Am | -0.080 | -0.162 | -0.017 | 0.116 | -0.017 |
| ²⁴² Cm | -0.188 | -0.009 | 0.026 | -0.019 | -0.186 |
| ²⁴³ Cm | 0.042 | 0.002 | -0.009 | -0.000 | 0.050 |
| ²⁴⁴ Cm | 0.161 | 0.086 | -0.041 | -0.0200 | 0.036 |
| ²⁴⁵ Cm | -0.068 | 0.006 | 0.029 | 0.004 | -0.106 |
| Total | -0.320 | -0.621 | -0.035 | 0.324 | -0.057 |

The delayed neutron fraction is connected operating and control of ADS. Moreover, monitoring of subcritical level in ADS is important because ADS must be subcritical in any case. The subcriticality is measured by units of β_{eff} in many experimental methods. The present status of delayed neutron data for major nuclides in evaluated nuclear data file is showed in Table 4. ENDF-B/VI contains data for all nuclides except for ²⁴⁴Cm. On the other hand, JENDL-3.2 and JEF-2.2 include only major Pu isotopes. Though JENDL-3.2 has part of delayed neutron data for all nuclides, complete set is necessary for evaluation of delayed neutron fraction. The contributions of these MA to delayed neutron fraction were investigated by calculation based on ENDF/B-VI library. As a result, it is about 30% for initial core and increase with fuel burnup. After five burnup cycles (about 10 years operation), it becomes about 60%. The complete set of these nuclides are desirable in future nuclear library from view point of MA transmutation system.

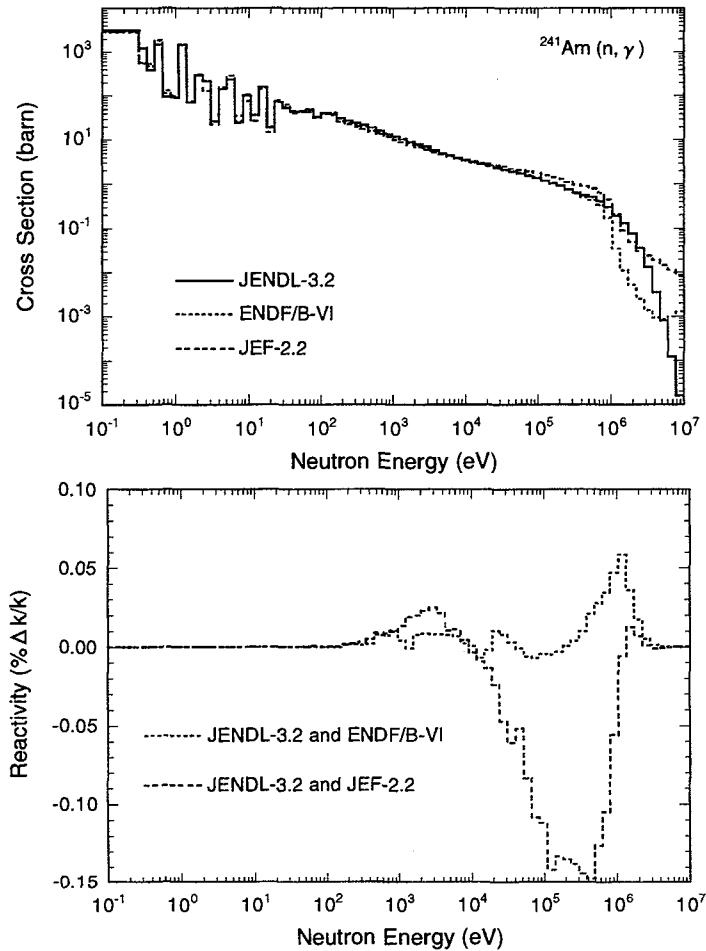


Fig. 3 $^{241}\text{Am}(n,\gamma)$ cross sections and energy break down of differences in capture reaction between nuclear data

For evaluation and improvement of nuclear data, not only differential experiments but also integrated experiments are indispensable. Actinide samples which were irradiated in the Dounreay Prototype Fast Reactor (PFR) are precious experimental data for MA.⁷ This experiment was done under a joint research program between the United States and the United Kingdom, a part of solution of sample were brought to JAERI from Oak Ridge National Laboratory. The samples were milligram quantities of actinide oxides of 21 different isotopes from thorium to curium that had been encapsulated in vanadium holders and exposed for 492 effective full-power days. The results of chemical analyses and comparison with calculational results are shown in Table 5. In Table 5, difference between beginning and ending of chemical analyses for main isotopes and fission per initial metal atom (FIMA) for samples are presented. The calculations were done by ORIGEN-2 code⁸ with JENDL-3.2 library. For difference during irradiation for main isotopes, the comparison with calculational results show good agreement with the experiments, except for ^{236}U , ^{238}Pu , ^{240}Pu and ^{242}Pu . For neptunium, americium and curium, there are large disagreement for FIMA while good agreement in difference for main isotopes. These results is preliminary one, so it will be needed more detailed calculation analysis to investigate the reason for these disagreement.

Some of fission products contained in residual waste from reprocessing have extremely long-term radiotoxicity. Partitioning and transmutation of the fission products are attracting considerable attention at present as an option to reduce the long-term radiological hazard of the

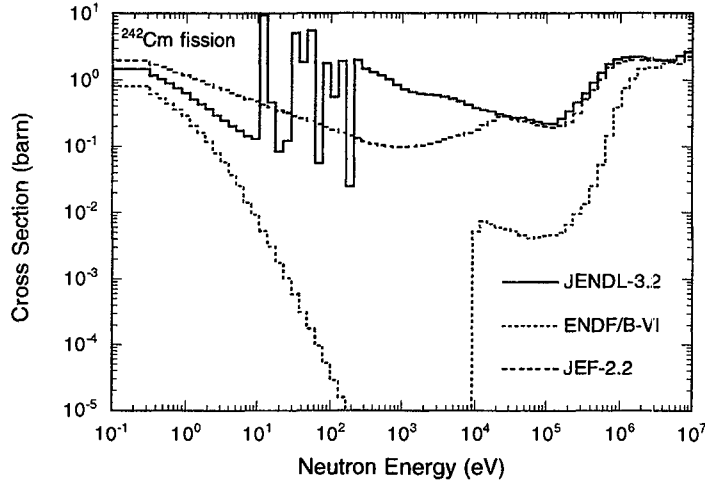


Fig. 4 ^{242}Cm fission cross section

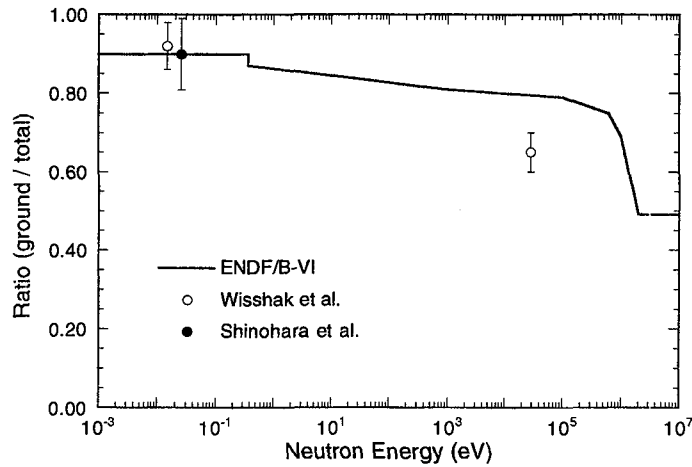
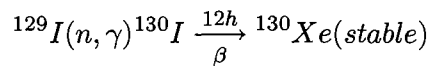
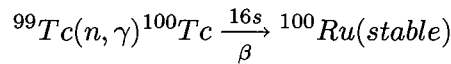


Fig. 5 Isomeric ration of $^{241}\text{Am}(n,\gamma)^{242g}\text{Am}$ and total $^{241}\text{Am}(n,\gamma)$ cross sections^{5,6}

high-level nuclear waste. After ^{137}Cs and ^{90}Sr are decayed out, the still remaining toxicities are from only the 7 LLFPs (^{79}Se , ^{93}Zr , ^{99}Tc , ^{107}Pd , ^{126}Sn , ^{129}I and ^{135}Cs). Among this 7 LLFPs, ^{99}Tc and ^{129}I are soluble in water and the most troublesome nuclides on the geological disposal technology, though these potential hazards are smaller than those of MA. In JAERI proposed system, for example, the Iodine are loaded axially and radially with the form of NaI around the MA-fuel core in ADS. It was shown that an ADS can transmute the MA and Iodine generated from about 10 units if LWR ^{99}Tc and ^{129}I become stable nuclide ^{100}Ru and ^{130}Xe according to following reactions.



Therefore, accuracy of capture cross section for ^{99}Tc and ^{129}I directly affect transmutation efficiency. Recent measured thermal cross sections (σ_0) and resonance integrals (I_0) in Japan

Table 4 Present state of delayed neutron data for major minor actinides in evaluated nuclear library

| | JENDL-3.2 | ENDF-B/VI | JEF-2.2 |
|---------|-----------|-----------|---------|
| Np-237 | △ | ○ | × |
| Pu-238 | △ | ○ | × |
| Pu-239 | ○ | ○ | ○ |
| Pu-240 | ○ | ○ | ○ |
| Pu-241 | ○ | ○ | ○ |
| Pu-242 | △ | ○ | × |
| Am-241 | △ | ○ | × |
| Am-242m | △ | ○ | × |
| Am-243 | △ | ○ | × |
| Cm-244 | △ | × | × |
| Cm-245 | △ | ○ | × |

○: all data exit,△: only ν_{di} and λ_i ,×: no data

Table 5 Results of chemical analyses on PFR-irradiated actinide sample and comparison with calculation results

| Sample | atom/IMA ^a | (C/E) | FIMA ^b (%) | (C/E) |
|-------------------|-----------------------|--------|-----------------------|--------|
| ²³³ U | -0.487 | (0.99) | 44.8 | (0.99) |
| ²³⁴ U | -0.185 | (0.96) | 9.19 | (1.06) |
| ²³⁵ U | -0.430 | (1.01) | 33.7 | (1.05) |
| ²³⁶ U | -0.100 | (1.33) | 5.93 | (1.09) |
| ²³⁸ U | -0.070 | (0.94) | 2.00 | (1.01) |
| ²³⁷ Np | -0.356 | (1.06) | 11.7 | (1.45) |
| ²³⁸ Pu | -0.453 | (1.15) | 21.9 | (1.34) |
| ²³⁹ Pu | -0.415 | (1.03) | 32.6 | (1.07) |
| ²⁴⁰ Pu | -0.206 | (1.12) | 10.9 | (1.14) |
| ²⁴¹ Pu | -0.504 | (1.01) | 28.4 | (1.13) |
| ²⁴² Pu | -0.158 | (1.20) | 6.25 | (1.10) |
| ²⁴¹ Am | -0.396 | (1.01) | 10.1 | (1.13) |
| ²⁴³ Am | -0.335 | (0.97) | 5.66 | (1.11) |
| ²⁴³ Cm | -0.365 | (0.97) | 31.0 | (1.18) |
| ²⁴⁴ Cm | -0.519 | (0.99) | 11.7 | (1.34) |
| ²⁴⁶ Cm | -0.084 | (0.97) | 8.45 | (1.24) |
| ²⁴⁸ Cm | -0.105 | (1.26) | 6.95 | (1.36) |

^a Difference between starting and ending atom per initial mass atom

^b Fission per initial mass atom

Nuclear Cycle Development Institute^{9,10} are shown in Table 6. Recent results of σ_0 is about 10% larger than the evaluated value. For resonance and keV region energy range, there is a few experimental data as shown in Fig. 6, so measurements with considerable precision are desired

Table 6 Thermal neutron capture cross sections (σ_0) and resonance integrals (I_0)

| $^{99}\text{Tc}(n,\gamma)^{100}\text{Tc}$ | | | | |
|---|-----|----------------------|-----------|--------------|
| | | $\sigma_0(\text{b})$ | | I_0 |
| Harada <i>et al.</i> ⁹ | '95 | 22.9 | ± 1.3 | 398 ± 38 |
| Lucas <i>et al.</i> ¹¹ | '77 | 20 | ± 2 | 186 ± 16 |
| JENDL-3.2 | | 19.65 | | 311.1 |
| ENDF/B-VI | | 19.57 | | 350.4 |
| JEF-2.2 | | 19.14 | | 304.2 |
| BROND-2 | | 19.14 | | 304.2 |

| $^{129}\text{I}(n,\gamma)^{130}\text{I}$ | | | | |
|--|-----|----------------------|-----------|----------------|
| | | $\sigma_0(\text{b})$ | | I_0 |
| Nakamura <i>et al.</i> ¹⁰ | '96 | 30.3 | ± 1.2 | 33.8 ± 1.4 |
| Roy <i>et al.</i> ¹² | '58 | 26.7 | ± 2.0 | 36.0 ± 4.0 |
| Block <i>et al.</i> ¹³ | '60 | 31 | ± 4 | |
| JENDL-3.2 | | 27.01 | | 28.98 |
| ENDF/B-VI | | 27.17 | | 35.56 |
| JEF-2.2 | | 33.93 | | 30.28 |
| BROND-2 | | 26.93 | | 27.97 |

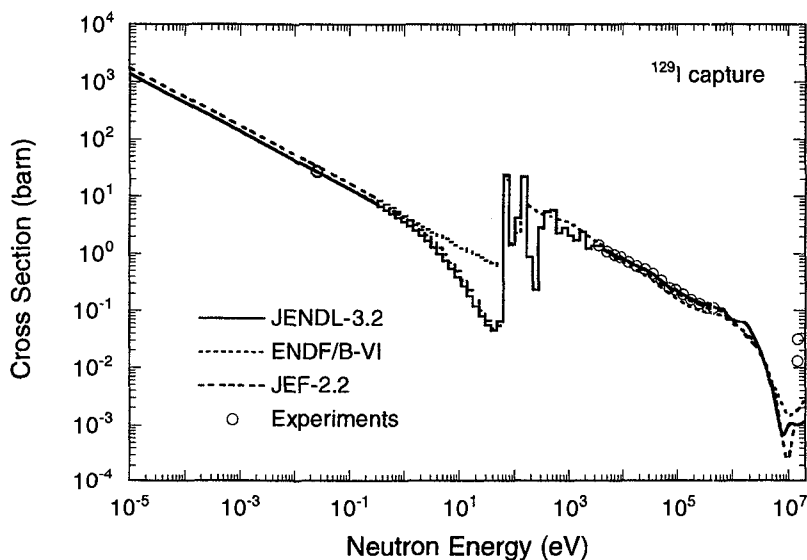


Fig. 6 ^{129}I capture cross section

3 Concluding Remarks

The conceptual design study of ADS are in progress at JAERI under the OMEGA program. Nuclides in high-level waste to be transmuted are MA and LLFP. JAERI proposed transmutation system for MA and LLFP was showed, and the effect of nuclear data for system characteristics, especially subcriticality and burnup swing, were investigated. From these results, the status of the evaluated data for the fission reaction is satisfactory for main nuclides in ADS, while large discrepancies are found in ^{242}Cm . The capture cross section are discrepant especially for ^{237}Np

and ^{241}Am . The importance of the nuclear data for secondary products MA, ^{238}Pu , ^{242m}Am and ^{245}Cm , are also showed. About ^{242m}Am , further investigation for the ratio of $^{241}\text{Am}(n,\gamma)^{242g}\text{Am}$ and $^{241}\text{Am}(n,\gamma)^{242m}\text{Am}$ reactions in higher energy region is needed. The present status of fission neutron yield, delayed neutron data and fission neutron spectrum in present evaluated nuclear data is not sufficient. For LLFP, recent measurement results for ^{99}Tc and ^{129}I which are the troublesome nuclides on the geological disposal were presented.

References

- [1] T.Takizuka, T.Sasa, K.Tsujimoto and M.Mizumoto, *Proc. Global '97*, vol.1 p.422 (1997).
- [2] K. Tsujimoto, T. Sasa, K. Nishihara, T. Takizuka, H. Takano, K. Hirota, Y. Kamishima, *Proc. ICONE-7* (1999).
- [3] "Calculations of Different Transmutation Concepts", OECD/NEA Nuclear Science Committee (2000).
- [4] T.Sasa, K.Tsujimoto, T.Takizuka and H.Takano, JAERI-Data/Code 99-007 (1999).
- [5] K. Wisshak, J. Wickenhauser, F. Kappeler, G. Reffo, F. Fabbri, *Nucl. Sci. Eng.*, **81**, 396 (1982).
- [6] N. Shinohara, Y. Hatsukawa, K. Hata, N. Kohno, *J. Nucl. Sci. Technol.*, **34**, 613 (1997).
- [7] B.D.Murphy, T.D.Newton and S.Raman, ORNL-6689 (1996).
- [8] A. G. Groff , ORNL-5621 (1980).
- [9] H. Harada, S. Nakamura, T. Katoh and Y. Ogata, *J. Nucl. Sci. Technol.*, **32**, 395 (1995).
- [10] S. Nakamura, H. Harada, T. Katoh and Y. Ogata, *J. Nucl. Sci. Technol.*, **33**, 283 (1996).
- [11] M. Lucas, R. Hagemann, R. Naudet, C. Renson and C. Chevalier, IAEA-TC-119/14, 407, (1977).
- [12] J. C. Roy and D. Wuschke, *Can. J. Chem*, **36**, 1424 (1958).
- [13] R. C. Block, G. G. Slaughter and J. A. Harvey, *Nucl. Sci. Eng.*, **8**, 112 (1955).